SLAC-PUB-7241
August, 1996

PHOTON DETECTORS WITH GASEOUS AMPLIFICATION

J. Va'vra
Stanford Linear Accelerator Center, Stanford University,
Stanford, CA 94309, U.S.A.

ABSTRACT

This paper reviews the progress of photon detectors with gaseous amplification over the last ten years.

Invited talk at the First Conference on Photon Detectors, Beaune, France June 24-28, 1996.

This work was supported by Department of Energy contract DE-AC03-76SF00515.

INTRODUCTION

J. Seguinot and T. Ypsilantis have described the theory and history of Ring Imaging Cherenkov (RICH) detectors at the Bari RICH workshop [1, 2]. At the Uppsala RICH workshop, a similar review was given by the author [3]; this discussed the various photon detector designs in greater detail, and included discussion of mistakes made, and detector problems encountered along the way. In this paper, the Uppsala paper is further expanded, while a careful effort is made to avoid repetition.

Gaseous photon detectors, including very large 4π-devices such as those incorporated in SLD and DELPHI, are finally delivering physics after many years of hard work. This success is due to the contributions of many people, but is also due to the pioneering work of J. Seguinot and T. Ypsilantis.

Photon detectors are among the most difficult devices used in physics experiments, because they must achieve high efficiency for photon transport and for the detection of single photo-electrons. Among detector builders, there is hardly anybody who did not make mistakes in this area, and who does not have a healthy respect for the problems involved. This point is stressed in this paper, and it is suggested that only a very small operating phase space is available for running gaseous photon detectors in a very large system with good efficiency and few problems.

In this paper we discuss what was done correctly or incorrectly in first generation photon detectors, and what would be our recommendations for second generation detectors. Examples of detectors belonging to the first generation are: DELPHI RICH [4], SLD CRID [5], OMEGA [6], etc. Examples of detectors belonging to the second generation are : RD-26 RICH detectors [7,8,9] or the Cornell RICH [10].

A major achievement of the first generation photon detectors was to convince the community that the RICH concept can be implemented to yield useful physics, since there were many skeptics in the early years of development. For example, after many years the SLD collaboration are finally "embracing" the CRID. However, pioneering work often results in mistakes. Some of these could not have been avoided because the necessary technology was simply unavailable in the early part of 1980's.

1. LESSONS LEARNED FROM THE FIRST GENERATION OF PHOTON DETECTORS.

First generation devices used drift time to measure the longitudinal coordinate. In order to resolve multiple hits, it was necessary to use a relatively short integration time constant (10-100 ns). Furthermore, the transverse coordinate detection methods, such as charge division or cathode pad reconstruction, coupled with the short charge integration constant, generally required a large total gas gain ($2\text{-}4\text{x}10^5$). In addition, many of these devices used a relatively thick TPC, which resulted in very large dE/dx deposits from charged particles traversing the

chamber. The high gas gain and large dE/dx deposits resulted in detrimental effects such as cross-talk, large photon feedback, wire ageing, self-sustaining currents, beam induced breakdowns and wire breakage (see chapter 4). For example, cross-talk and photon feedback due to large dE/dx signals reduce the particle identification capability in the dense core of a jet. Wire ageing and self-sustaining cathode currents may cause a general deterioration of the detector, especially in detectors operating in a large background environment.

In fact, a very small operating phase space is available for running gaseous photon detectors in a very large system, with good detection efficiency and few problems over a period of years. This point is now explored in more detail.

1.1. Choice of gas gain.

One should be "very gentle" with the choice of gas gain. A detector design must be electrostatically clean before the photosensitive materials are introduced, because they tend to further amplify any weak feature of the design. This means that the maximum allowed dark cathode current must be less than 1 nA. It should be also assumed that the performance of the detector will deteriorate somewhat after many years of operation, often in harsh background conditions. For example, the CRID detectors, which have operated with TMAE for five years now, do not reach the same maximum operating voltage as initially. The reality of such limitations should prompt one to make a compromise regarding how far one wants to push the detection efficiency. Fig. 1 shows an example of the calculated single electron efficiency, ε, for several electronics thresholds. The calculation is based on fitting the Polya distributions measured with the UV calibration single photon source in CRID [3]. The calculated single electron efficiency for a known threshold, Th, is given by:

$$\varepsilon = \int_{Th}^{\infty} P(q)\,dq \Big/ \int_{0}^{\infty} P(q)\,dq\,, \qquad (1)$$

where $P(q)$ is the Polya function. The present CRID operating point corresponds to a single electron efficiency of about 85-90%. This may seem low; however, there are limiting factors. On the one hand, the gas gain is limited by possible detector problems (see chapter 4), while on the other, the electronics threshold cannot be reduced. For a threshold of ~1.5×10^4 e^-, which is suitable for taking UV fiber generated single electron data, the anode wire detection efficiency is ~95%. However, when running the hadronic Z trigger, which has a high number of tracks with large dE/dx charge deposits, the threshold must be raised to ~$2\text{-}3\times10^4$ e^- in order that the total number of hits should fit into the system buffer. Figures 2 and 3 show the cross-talk problems of the SLD CRID [5] and DELPHI detectors [11]: a complicated recovery of the CRID charge amplifier from very large dE/dx pulses causes spurious hits. Similarly, the DELPHI detector, operating with a current amplifier with a short integration time (10-20 ns), has to run at high gas

gain to obtain an acceptable cathode pad efficiency; this, in turn, contributes to large cross-talk for large dE/dx pulses. Extra hits can be removed by various software cleaning schemes, but not without some loss of N_O, especially in the core of a jet.

Operation at high gas gain causes extra hits from avalanche feedback photons. Such hits confuse the reconstruction in the core of a jet. Fig. 4 shows how the detectors of the first generation solved the photon feedback problem in TMAE laden gases. Although such complicated electrode blind structures reduce extra hits in the TPC volumes, they do nothing to eliminate other detector problems (see chapter 4). One may ask what gas gain is necessary to eliminate the need for such complicated electrode structures. Fig. 5 shows the rate of secondary photo-electrons per avalanche as a function of total avalanche charge in two geometries of the CRID detector, with and without the electrode blinds. To run the geometry without the blinds and have the rate of secondary after-pulses below 1% requires the total gas gain to be ~$8x10^4$ or less [12]; first generation detectors had a typical total gas gain 2-$4x10^5$, i.e. typically five times more. In ref. 12 it is shown also that the avalanche feedback rate depends on the total avalanche charge, and not on the anode wire diameter (the wire diameter controls the value of the electric surface field).

1.2. Choice of charge integration time constant.

The induced charge on any electrode in a wire chamber is a complicated function of the electrostatic configuration, geometry, integration time of the amplifier, etc. [13,14]. In addition to a discussion presented in Ref. 3, I would like to add one example from CRID, which illustrates the need for a careful choice of integration time constant. Fig. 6 shows a calculation of the pulse waveform on a CRID amplifier for two cases: a 65 ns (present CRID value) and a 20 ns long charge integration time of the amplifier. The calculation was done for 7 μm diameter anode wire and ethane gas. The peak amplitude is severely reduced in the latter case. To recover the peak amplitude in the 20 ns case, cathode voltage would have to be increased by ~150 Volts, which would probably cause problems.

Another example is the Fast RICH MWPC chamber with cathode pad readout. For short integration times, the size of the induced charge on the cathode is considerably smaller than that at the anode. To compensate for the lower signal on the cathode, a very small anode-cathode spacing must be chosen, and the chamber must be operated at higher gas gain. This in turn increases the cathode surface gradients, which may be relevant for CsI photo-cathode solutions. Very short integration times are necessary in high rate experiments at LHC, consequently gaseous photon detector applications will be more difficult to implement there. However, in many applications, such as the B-factory or low rate applications at LHC, the occupancy rate per pad is small, so that a very long integration time can be used. For example, the AMPLEX chip [15], as used by the RD-26 prototypes [7,8,9], has integration time ~600 ns , and the VIKING

chip [16], as used in the Cornell prototype [10], has integration time ~1μsec. With such electronics, it is possible to operate with total gas gain below ~10^5, since, for such long integration time constants, more charge is available, and the electronic noise is smaller.

2. RECOMMENDATIONS FOR THE SECOND GENERATION OF PHOTON DETECTORS.

Second generation devices should trade high gas gain (2-5x10^5), short charge integration constant (10-100 ns) and drift time measurement, for small gas gain (~5x10^4), long charge integration constant (600-1000 ns), low noise electronics (< 500 e^- rms), and geometrical pixelization. In addition, the detectors should be thin. In principle, all three photo-cathodes, i.e. TMAE, TEA and CsI, can be used in this approach, although in the case of TMAE it means a hot TMAE bubbler temperature (~35°C). Detector operation at very low total gas gain results in an exponential pulse height spectrum; the only way to have good single electron detection efficiency (>95%) under such conditions is to have very low noise electronics (~500 e^- rms). The new electronics developments at CERN, such as the GASSIPLEX and FELIX chips, will be important for the second generation of gaseous photon detectors.

The above recommended recipe will not be adequate for high rate applications of RICH detectors at the LHC. At the moment, there is no working solution for gaseous detectors in this environment.

3. EXAMPLES OF DETECTORS USED FOR CHERENKOV PHOTON IMAGING.

Ref. 3 discussed in detail many gaseous photon detectors, grouping them into the following major categories:

A. RICH using "LONG" drift:

DELPHI prototype[17], DELPHI [4], SLD CRID[5], OMEGA[6], UA2-RICH [18].

B. RICH using "SHORT" drift:

Fast Drift CRID prototype [19].

C. RICH using "FAST" MWPC :

a) with "FAST" electronics:

CERES [20], College de France - "TEA and CsI" prototypes [21], HERA-B "CsI" prototype [22];

b) with "SLOW" electronics:

RD26 (Munich, Saclay, CERN) for HADES, BaBar and ALICE [7,8,9],
Princeton prototype for KEK [24], Cornell prototype[10], CAPRICE [25], RICH-II (Chicago) [26], CDF CsI prototype [27].

D. RICH with "SPECIAL" operation or geometry:

a) with "SPECIAL" geometry :

JETSET[28], HERA-B "TMAE" prototype[23], College de France - "TMAE" prototype [29];

b) with "LOW" pressure operation :

HELIOS "TMAE" pad prototype [30], PHENIX prototype[31];

c) with "OPTICAL" readout:

HELIOS "TMAE" prototype [32], NA35 prototype[33].

E. RICH with micro-strip, micro-gap and micro-dot chambers:

Munich [34], INFN Pisa [35], Weizmann [36], Liverpool prototypes [37].

The entire discussion of Ref. 3 will not be repeated; instead, several developments which have occurred since the Uppsala RICH workshop will be mentioned:

Two HERA-B prototypes, based on CsI [22,23] and TMAE [23] photo-cathodes, were rejected in competition with a PM-based photo-detector. The CsI prototype detected only half the expected number of photo-electrons, and the TMAE based prototype detected only one quarter. In addition, the TMAE chamber confirmed the existence of wire ageing problems, and the CsI test chamber detected the presence of self-sustaining currents during high rate tests. On the other hand, tests with the Hamamatsu #6568 PM showed very encouraging results in a high background environment.

Similarly, the College de France "TMAE" [29] prototype, intended for medium-rate applications, achieved poor electron transmission through its blind structure.

However, there has been progress in the area of detectors with CsI photo-cathodes working in conditions where lower rates are expected. The TIC detector in the NA44 experiment demonstrated, for the first time, the physics capabilities of such a photo-cathode.

There has not been much progress in the area of micro-strip or micro-gap gaseous photon detectors since the Uppsala workshop. Perhaps it is unrealistic to expect much progress as long as the aim is large gas gain operation ($>10^5$). Recently, a similar scheme was proposed in the form of the micro-dot detector [37] (see Fig. 7). Instead of strips, the chamber uses cathode rings. A gas gain of $3\text{-}4\times10^4$ was achieved in a 50% Ar+50% DME mixture. The authors hope that this detector geometry will detect single electrons using the FELIX electronics chip, and that it could be used for some LHC photon detector applications. The microdot diameter is 20 μm . It is important to use a diameter which is sufficiently large that the avalanche has a sufficient number mean free paths. Fig. 8 shows a micro-needle detector [38] which did not work because the needles had a diameter much less than 1 μm . The electric field changes so rapidly that the avalanche electrons do not have a sufficient number of mean free paths available, and so no gain is observed at normal pressure[38]. A simulation of this problem is given in Ref. 39, which suggested operating at higher gas pressure. I would add that, perhaps, a liquid could be tried.

4. EXAMPLES OF PHOTON DETECTOR PROBLEMS.

Many effects mentioned in this chapter are related to the choice of very high gas gain, a common feature of first generation photon detectors. If the gas gain were decreased by a factor of 5, many of these effects would become less significant. The entire discussion of Ref. 3 will not be repeated here; instead, only new developments since the Uppsala workshop will be mentioned.

4.1. Wire ageing (anode related effects).

A high rate of polymerization is expected in TMAE-laden gases because the low mean ionization potential of the TMAE molecule (5.4 eV) provides the photo-ionization capability, and because the N-CH_3 bond strength is less than 3 eV, which results in a high degree of fragility. The polymerization deposits are good insulators , and cause a drop in wire gain, with subsequent loss of efficiency. A large gain drop was observed in early R&D tests [40], and was subsequently confirmed in different test configurations [41,42,43,23]. The early tests [40] found a number of interesting dependencies : (a) the wire ageing rate decreased with an increase in the complexity of the hydrocarbon molecule of the carrier gas; (b) it decreased with an increase in the diameter of the anode wire; (c) it did not seem to depend on TMAE concentration, gas flow, anode material, detector temperature, or source intensity; (d) the anode wire deposit appeared to consist of a thin film which reacted with air to form droplets after the chamber was opened (these droplets could be easily washed away using alcohol, but if left on the wire, they would slowly increase in viscosity, and after a year would have the consistency of honey); (e) the anode wire ageing deposits could be evaporated easily by passing a small current of about 10 mA in the case of 7 μm diameter carbon wire.

To date, most large experiments have accumulated a negligible charge dose, and so are unable to confirm the test results directly. In fact, in most cases wire ageing is not yet a problem. However, high rate or thin wire applications have seen these effects already. The SLD CRID, which uses very thin 7 μm diameter anode wires, has observed a gain drop of about 25% in the running period between 1993 and 1996, while accumulating a charge dose of about 0.01-0.1 mC/cm of wire length; Fig. 9a shows the gain drop in one TPC. A slight recovery occurred before the 1996 run; this is believed due to long term flushing with nitrogen (~11 months). It should be noted also that the gain drop rate in the 1996 run was smaller than measured previously; this is believed to be due to cleaner running conditions. Fig. 9b shows an example of full gain recovery after one detector was removed, and its cathode and wires were washed in ethanol; this result is consistent with the early R&D [40]. Similarly, the OMEGA RICH [23] observed a very large gain drop in the 1991 run after a charge dose ~1 mC/cm. Recently, the CERES detector [44] observed wire deposits, and the HERA-B "TMAE" prototype[23, 45] measured a large gain drop consistent with the early measurements [40].

Very recently, a comparison between TMAE and TEA wire ageing has been performed in a high rate test setup [46]. The results indicate that: (a) the TEA wire ageing rate (20% gain drop) appears to be slower than that of TMAE by a factor of 4-7; (b) the TEA wire ageing rate is inversely proportional to the anode wire diameter; (c) a TEA-aged anode wire surface may be regenerated by means of the heating which accompanies the passage of a small current through the wire; this is similar to TMAE. Fig. 10 shows the comparison of TEA and TMAE anode wire ageing.

4..2. Cathode related effects.

All photosensitive materials, and, very probably, their various ageing deposits, are good insulators. In the presence of a large background, positive ions deposited on the cathode surface may cause a large increase in the electric field across such an insulating layer, and this, in turn, may cause emission of electrons from the cathode, i.e. the well-known Malter effect [47]. What is not often realized is that the detector may operate in a mode where such currents are excited momentarily, but decay quickly in time. Such behavior is very difficult to observe, because the high voltage current trip is usually set higher than the magnitude of this effect. It took a great deal of detective work to discover such an effect in the SLD CRID detectors [48]. They operate with very thin wires of 7 μm diameter, which may enhance such effects due to a larger positive ion concentration (smaller avalanche size).

It is natural to ask if similar effects could exist in CsI-based chambers. Recently, the volume resistivity of the CsI film was measured [49], and its value found to be between 10^{11} and 10^{12} Ωcm. This gives a protection of 3-4 orders of magnitude, if the volume resistivity remains stable over the lifetime of an experiment.

In ref. 46 it is shown that it is possible to excite a self-sustaining cathode current condition even in a TEA-based detector, if it operates at a gas gain of 2-3x10^5; in one case in ~12 tries a current persisted even after the source was removed.

4.3. Quenching and sparking.

A cathode next to anode wires can be coated either directly (CsI) or indirectly (TMAE, TEA, wire ageing deposits of TMAE, etc.) by a photosensitive material. The avalanche photons can cause emission of secondary photoelectrons. If the efficiency of this process, η, and the <u>total</u> gas gain, G, are high enough that η.G~1, the chamber goes into a self-sustaining current mode, and becomes very unstable. If η is small, such photoelectrons cause extra noise only, and this problem can be solved by a suitable choice of electrode blind structure (see Figs. 5, 6). However, a better way to deal with this problem in future would be to choose: (a) <u>lower gas gain</u>, (b) a structure which allows only small primary charge deposits (a <u>thin</u> detector or <u>low pressure</u> operation), and (c) a <u>suitable gas</u> (for example iC_4H_{10}). The advantage of the TEA-based photo-

cathode in this respect is a very short photon absorption length (ℓ_{abs}~0.6 mm), which limits the effect of avalanche photons, and allows a thin detector structure.

If the number of primary ion pairs, $N_{prim.ion.}$, and the <u>total</u> gas gain, G, are such that the condition $N_{prim.ion.}.G>10^8$ is satisfied, the chamber will spark. This is the well-known Raether condition [50], derived 40 years ago, and recently rediscovered in our field [51].

4.4. Solid photo-cathodes.

Solid photo-cathodes, such as CsI, are not without possible problems either [52]. Photo-cathode damage may occur: (a) by light exposure only (no gain), (b) by gas gain, (c) by sparking, (d) by environmental damage due to gas-related effects such as air exposure, temperature, etc., and (e) by an "electrolytic" current through the volume causing the plating of the ionic species on various electrodes. In my opinion, the last point is the most important. It is well known that the ionic species migrate under the influence of the potential in alkali halides [53]; Cs^+ ions will migrate to the surface in a typical Fast RICH detector with pad structure, and similarly, Cs^+ and I^- ions will migrate to cathode and anode respectively in micro-strip detectors operating in reflective mode. For example, after only one week of running with 100 Volts across the anode-cathode micro-strip structure covered by the CsI photo-cathode, plating deposits were clearly observed on the anode electrode after it was exposed to air (the deposits are believed to be iodine) [49].

There is a rather large variation in recent CsI ageing results. For example, the CsI photo-cathode ageing in a MWPC chamber, operating with 1 atm CH_4 at a total gas gain ~10^5, resulted in a 20% photo-current loss after [49]: (i) a charge dose of only ~1 $\mu C/mm^2$ using a stainless steel substrate, and limiting the total accumulated charge dose to only ~3 $\mu C/mm^2$; (ii) a charge dose of ~6-8 $\mu C/mm^2$ using a copper-clad PCB covered with the Sn/Pb alloy, and limiting the total accumulated charge dose to only ~10 $\mu C/mm^2$; and (iii) a charge dose of ~90 $\mu C/mm^2$ using a copper-clad PCB chemically covered with Ni and Au, and limiting the total accumulated charge dose to only ~100 $\mu C/mm^2$. This is to be compared with results from different tests indicating equivalent charge doses of ~80 $\mu C/mm^2$ [54], and ~15 $\mu C/mm^2$ [55]. Recently, a rapid decrease in the photo-current, followed by a fast rise and subsequent slow decay was observed (see Fig. 11); similar behavior was reported in Ref. 49. Clearly, more work is needed in this area.

5. A TMAE, TEA or CsI-BASED PHOTO-CATHODE ?

The following provides a brief summary of basic considerations when comparing various photo-cathode materials:

1. The TMAE photo-cathode: (a) still gives the highest QE of all photo-cathode materials, (b) is continuously "refreshing", (c) is difficult to clean, (d) does not tolerate gas system accidents,

(e) requires a "thick" detector for "low" temperature operation (the only way to make a "thin" detector is to run the TMAE bubbler at 35-40°C, and the detector at 40-45°C), (f) requires an extra front window, (g) gives the most severe wire ageing. There is now substantial experience with long term running of TMAE-based detectors.

2. The TEA photo-cathode: (a) allows a "thin" detector operating at ambient temperature, (b) is continuously "refreshing", (c) requires more expensive MgF_2 windows, (d) gives better wire ageing properties than TMAE. There is no experience with long term running of TEA-based detectors.
3. The CsI photo-cathode: (a) allows a "thin" detector operating at ambient temperature, (b) is not continuously "refreshing", (c) cannot be exposed to air for a long time, (d) has ageing properties which are not understood at present. There is no experience with long term running of CsI-based detectors.

CONCLUSIONS

The detection of single electrons using gaseous devices is rather tricky. To many involved in the planning of large experiments, it was not clear initially whether it would be possible to detect single photo-electrons on such a large scale with good efficiency. It has required a great deal of effort to make such systems perform effectively, and many mistakes have been made along the way. Drift chambers and TPC's, which are commonly used today for tracking, have required many iterations to become successful and accepted. If a similar number of iterations were allowed for the evolution of gaseous photon detectors, they would improve, and prove themselves to be reliable particle identification devices. Considering that photon detectors have finished only their first iteration, they have performed remarkably well, especially in fixed target applications. I would add the following comments :

A. Single electron detection on a very large scale using gaseous photon detectors has been demonstrated to be effective, even in large 4π detectors.
B. There is very small phase space available for the operation of gaseous photon detectors with good efficiency and reliability over a period of several years.
C. For second generation photon detectors it is recommended that they operate with:
   a) as low gas gain as possible ($2\text{-}4 \times 10^4$),
   b) that they be "thin" detectors in order to minimize dE/dx deposits,
   c) that they incorporate pad readout with a long integration constant (for "non-LHC or low-rate-LHC applications").
   d) that they try to incorporate microdot detector geometry (for "high-rate-LHC applications").
D. Only new ideas will "save" gaseous detectors from extinction in the "high rate age."

ACKNOWLEDGMENTS

I would like to thank the organizers of the conference, especially P. Besson, for providing a very interesting and stimulating experience.

FIGURE CAPTIONS

1 The calculated single electron efficiency for several electronics thresholds; the calculation is based on fitting the Polya distributions measured with UV fiber calibration pulses in CRID [3].

2. The complicated recovery of the CRID charge amplifier from very large dE/dx pulses causes spurious hits [5].

3. To obtain acceptable cathode pad efficiency, the DELPHI detector [4] must operate at high gas gain, which results in large cross-talk for large dE/dx pulses. Extra hits can be removed by various software cleaning schemes, but not without some loss of N_O.

4. The electrode blinds used in TMAE-based detectors for : (a) the DELPHI prototype [17], (b) the DELPHI barrel [4], (c) the CRID barrel [5] and (d) the OMEGA experiments [6].

5. The rate of secondary photo-electrons per avalanche as a function of total avalanche charge for the CRID detector with and without electrode blinds [12], and in TMAE-laden ethane.

6. The calculated pulse waveforms for a CRID amplifier with charge integration times of 65 and 20 ns (7 μm diameter anode wire and ethane gas).

7. The concept of the micro-dot detector [37]; the microdot diameter is 20 μm .

8. The concept of the micro-needle detector [38]; no observable gas gain was measured at normal pressure, even in DME gas, due to the extremely thin radius of the needle ($<<$ 1 μm).

9. Wire ageing in the SLD CRID between 1993 and 1996 with: (a) a detector, which was never removed, and (b) a detector which was removed after the 1995 run and washed in ethanol. The average pulse height is monitored using the UV fiber single photon calibration pulses.

10. Wire ageing test results with, (a) C_2H_6+TMAE and C_2H_6+TEA for wire diameter 20 μm, and (b) with C_2H_6+TEA for anode wire diameters 7, 20 and 33 μm [46].

11. CsI photo-cathode ageing in a MWPC chamber operating with 1 atm CH_4 at a total gas gain ~10^5 [56]; the photo-cathode was damaged by the UV Cherenkov photons created by β-electrons from a Sr^{90} source [56].

REFERENCES

[1] J. Seguinot and T. Ypsilantis, Nucl.Instr.&Meth., A343(1994)1.

[2] J. Seguinot and T. Ypsilantis, Nucl.Instr.&Meth., A343(1994)30.

[3] J. Va'vra, Nucl.Instr.&Meth., A371(1996)33.

[4] D. Bloch et al., Nucl.Instr.&Meth., A273(1988)847; W. Adam et al., Nucl.Instr.& Meth., A343(1994)68; M. Darkos and D. Loukas, Nucl.Instr.&Meth., A302(1991)241, W. Adam et al., Nucl.Instr.&Meth., A338(1994)284; W. Adam et al., Nucl.Instr.&Meth., A371(1996)12.

[5] D. Aston et al., Nucl.Instr.&Meth., A283(1989)582; K. Abe et al., Nucl.Instr.&Meth., A343(1994)74; K. Abe et al., Nucl.Instr.&Meth., A371(1996)195; K. Abe et al., Nucl.Instr.&Meth., A371(1996)8.

[6] H.-W. Siebert, Nucl.Instr.&Meth., A343(1994)60; U. Muller et al., Nucl.Instr.&Meth., A371(1996)27; S. Abatzis et al., Nucl.Instr.&Meth., A371(1996)22.

[7] F. Piuz, Nucl.Instr.&Meth., A371(1996)96; A. Bream et al., Nucl.Instr.&Meth., A343(1994)163.

[8] P. Besson, private communication; R. Aleksan et al., Nucl.Instr.&Meth., A343(1994)173.

[9] R. Gernhauser et al., Nucl.Instr.&Meth., A371(1996)300; J. Friese, presentation at this conference.

[10] S. Playfer et al., Nucl.Instr.&Meth., A371(1996)321.

[11] D. Bloch, M. Darcos and S. Tzamarias, Nucl.Instr.&Meth., A371(1996)236.

[12] K. Abe et al., Fifth International Conference on Instrumentation for Colliding Beam Physics, Novosibirsk, Russia (March 15, 1990).

[13] E. Gatti, P.F. Manfredi, V. Radeka, Riv. Nuovo Cimento 9(1986), and Ann. Rev. Nucl. Part. Sci. (1988)217.

[14] R. Bellazzinni and M.A. Spezziga, Riv. Nuovo Cimento 12(1994).

[15] E. Beuville, K. Borer, E. Chesi, E.H.M. Heijne, P. Jarron, B. Lisowski and S. Singh, Nucl.Instr.&Meth., A288(1990)157.

[16] E. Nygard, P. Aspell, P. Jarron, P. Weilhammer and K. Yoshioka, Nucl.Instr.&Meth., A301(1991)506.

[17] R. Arnold et al., Nucl.Instr.&Meth., A270(1988)255.

[18] O. Botner et al., Nucl.Instr.&Meth., A257(1987)580; L.O. Eek et al., IEEE Trans. Nucl. Sci., NS 31 (1984)949; K. Fransson, Ph.D. thesis, ISBN 91-7900-908-4, Uppsala (1990).

[19] J. Va'vra, SLAC B-Factory note #68 (1994).

[20] R. Baur et al., Nucl.Instr.&Meth., A343(1994)87, and Nucl.Instr.&Meth., A343(1994)231.

[21] J. Seguinot et al., Nucl.Instr.&Meth., A350(1994)430; R. Arnold et al., Nucl.Instr.&Meth., A314(1992)465; M. French et al., Nucl.Instr.&Meth., A324(1993)511;

J. Seguinot et al., Nucl.Instr.&Meth., A371(1996)64.
[22] J. Krizan et al., Nucl.Instr.&Meth., A371(1996)151;
J. Staric et al., presentation at this conference.
[23] T. Hamacher et al., Nucl.Instr.&Meth., A371(1996)289;
J. Staric et al., presentation at this conference.
[24] C. Lu et al., Nucl.Instr.&Meth., A371(1996)155.
[25] P. Carlson et al., Nucl.Instr.&Meth., A343(1994)198;
G. Barbiellini et al., Nucl.Instr.&Meth., A371(1996)169.
[26] S. Swordy, private communication; J. Buckley et al., The Astrophysical Journal, 429 (1994) 736; S. Swordy, Nucl.Instr.& Meth., A343(1994)52.
[27] W. Kononenko and N.S. Lockyer, Nucl.Instr.&Meth., A371(1996)143.
[28] R.T. Jones, M. Price and H. Wirth, Nucl.Instr.&Meth., A343(1994)208.
[29] J. Seguinot et al., private communication.
[30] A. Fisher et al., IEEE Trans.Nucl.Sci., 35(1988)432.
[31] B. Surrow et al., Nucl.Instr.&Meth., A355(1995)342.
[32] A. Breskin et al., Nucl.Instr.&Meth., A273(1988)798, and IEEE Trans.Nucl.Sci., 35(1988)404.
[33] J. Baechler et al., Nucl.Instr.&Meth., A324(1993)449, and Nucl.Instr.&Meth., A343(1994)288.
[34] K. Zeitelhack et al., Nucl.Instr.&Meth., A371(1996)57.
[35] R. Bellazzini, private communication; see also Ref. 3.
[36] E. Shefer, private communication; see also Ref. 3.
[37] S. Biagi et al., Nucl.Instr.&Meth., A366(1995)76, and Nucl.Instr.&Meth., A361(1995)72;
S. Biagi, private communication.
[38] J. Va'vra, L. Madansky, S. Williams, SSC proposal, (August 30, 1988); the micro-needle concept was described in a paper by C.A. Spindt et al., Journal of Appl. Physics, 47(1976)5248.
[39] D. Mattern and M. C. S. Williams, CERN internal note, (January, 1991).
[40] J. Va'vra, IEEE Trans. Nucl. Sci., NS34(1987)486; CRID Note #36, SLAC (1987); IEEE Trans. Nucl. Sci., NS 35(1988)487; Nucl.Instr.&Meth., A367(1995)353.
[41] C. Woody, IEEE Trans. Nucl. Sci., NS 35(1988)493.
[42] J. Va'vra, J. Kadyk, J. Wise and P. Coyle, SLAC-PUB-95-6783, and Nucl.Instr. &Meth., A324(1993)113.
[43] K. Martens et al., Nucl.Instr.&Meth., A343(1994)258.
[44] I. Tserruya, private communications.
[45] P. Krizan, private communication.
[46] J. Va'vra, contribution to this conference, and SLAC-PUB-7168 (1996).

[47] L. Malter, Phys.Rev. 50(1936); A. Guentherschulze, Z.Phys. 86(1933)778.
[48] J. Va'vra, Nucl.Instr.&Meth., A367(1995)353.
[49] J. Va'vra, A. Breskin, A. Buzulutskov, R. Chechik, and E. Shefer, contribution to this conference, and SLAC-PUB-7095 (1996).
[50] H. Raether, Z. Phys. 112(1939)464.
[51] P. Fonte, V. Peskov and F. Sauli, Nucl.Instr.&Meth., A305(1991)91.
[52] A. Breskin, Nucl.Instr.&Meth., A371(1996)116.
[53] N.W. Ashcroft, N.D. Mermin, Solid State Physics, p. 621, N.Y., Holt, Rinehart and Winston (1976).
[54] P. Krizan et al., IJS report, IJS-DP-7087 (1994).
[55] C. Lu et al., Princeton preprint HEP/95-1.
[56] P. Krizan, private communication.

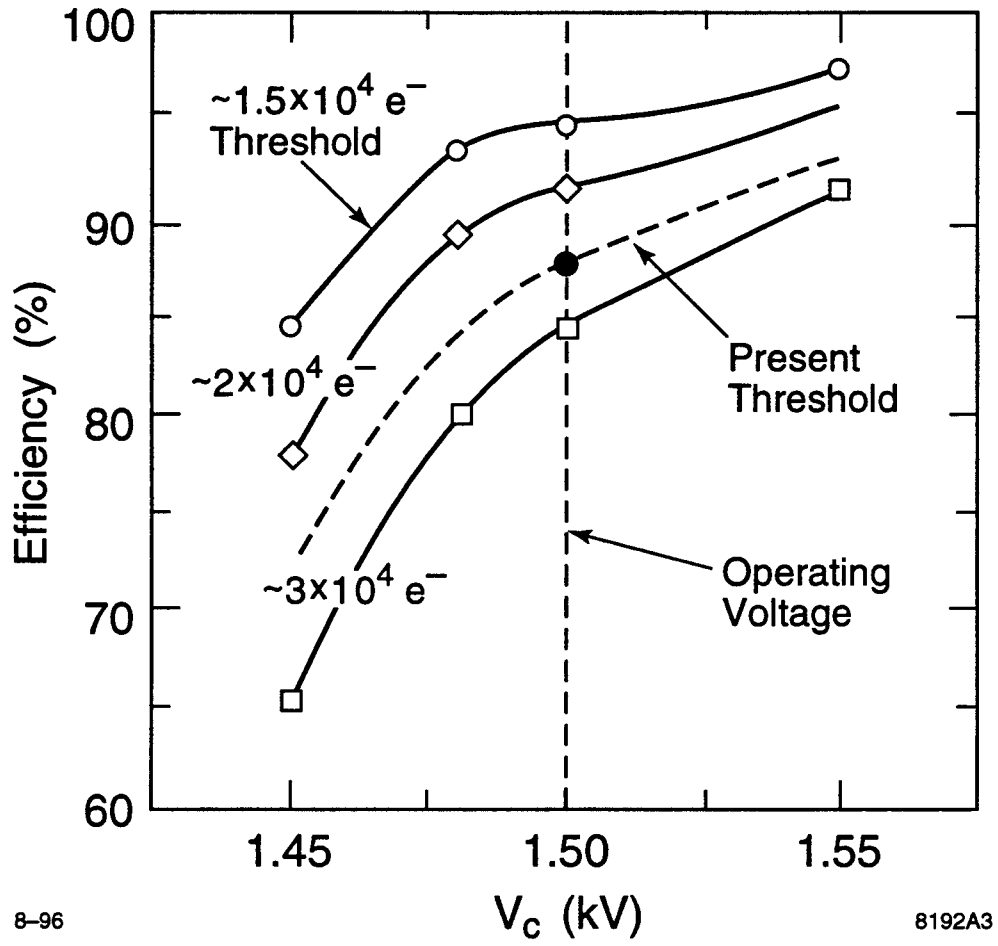
100
90
80
70
60
Efficiency (%)
~1.5x10^4 e^-
Threshold
~2x10^4 e^-
~3x10^4 e^-
Present
Threshold
Operating
Voltage
1.45
1.50
1.55
Vc (kV)
8–96
8192A3

Fig. 1

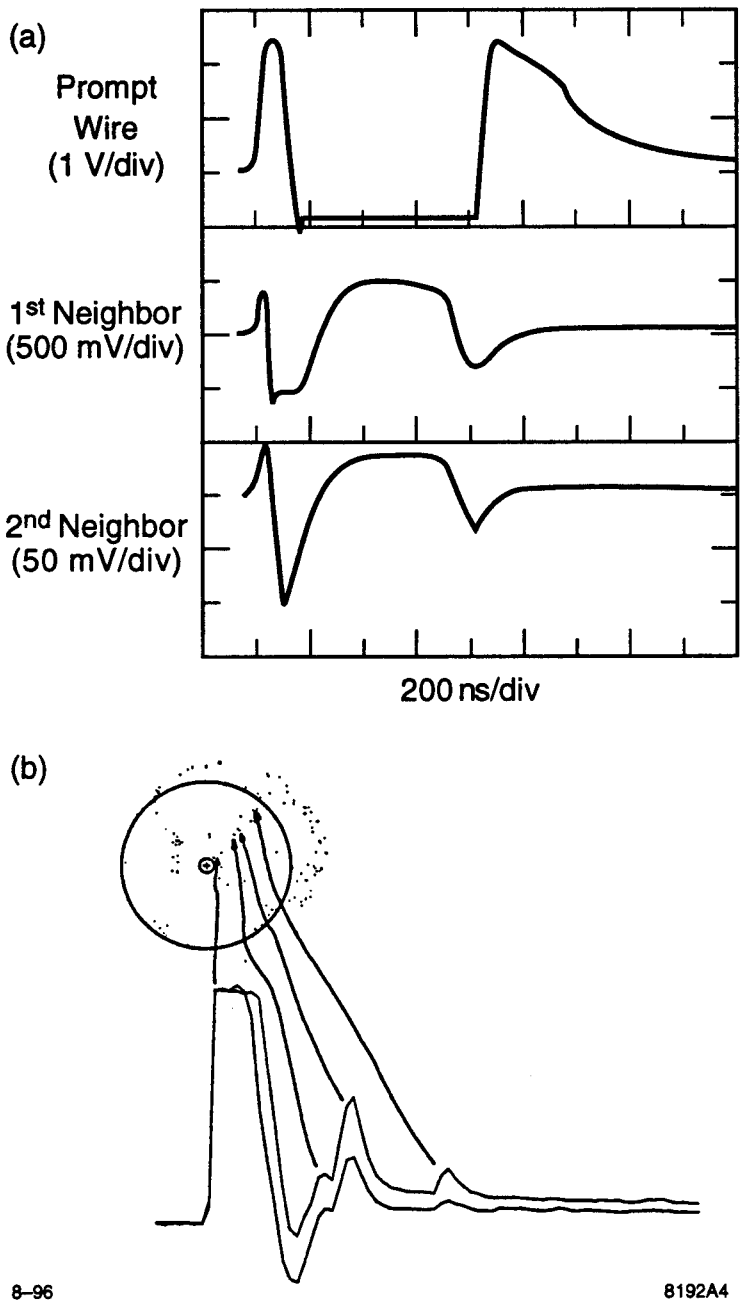
(a)
Prompt
Wire
(1 V/div)
1st Neighbor
(500 mV/div)
2nd Neighbor
(50 mV/div)
200 ns/div
(b)
8–96
8192A4

Fig. 2

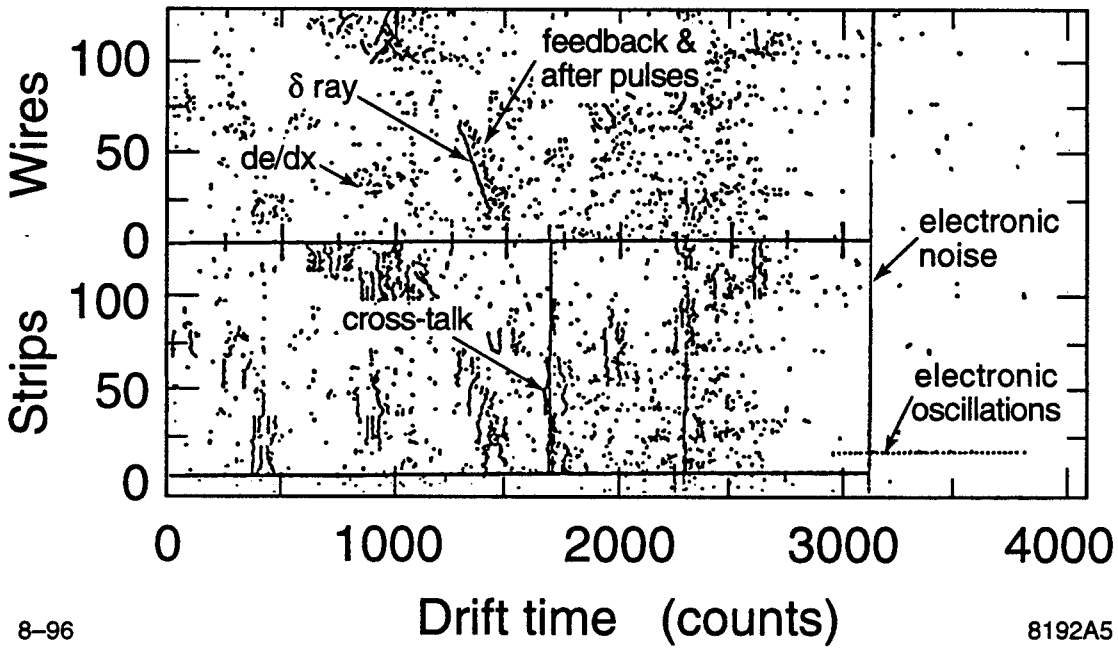
Wires
100
50
0
Strips
100
50
0
feedback &
after pulses
δ ray
de/dx
electronic
noise
cross-talk
electronic
oscillations
0
1000
2000
3000
4000
Drift time (counts)
8–96
8192A5

Fig. 3

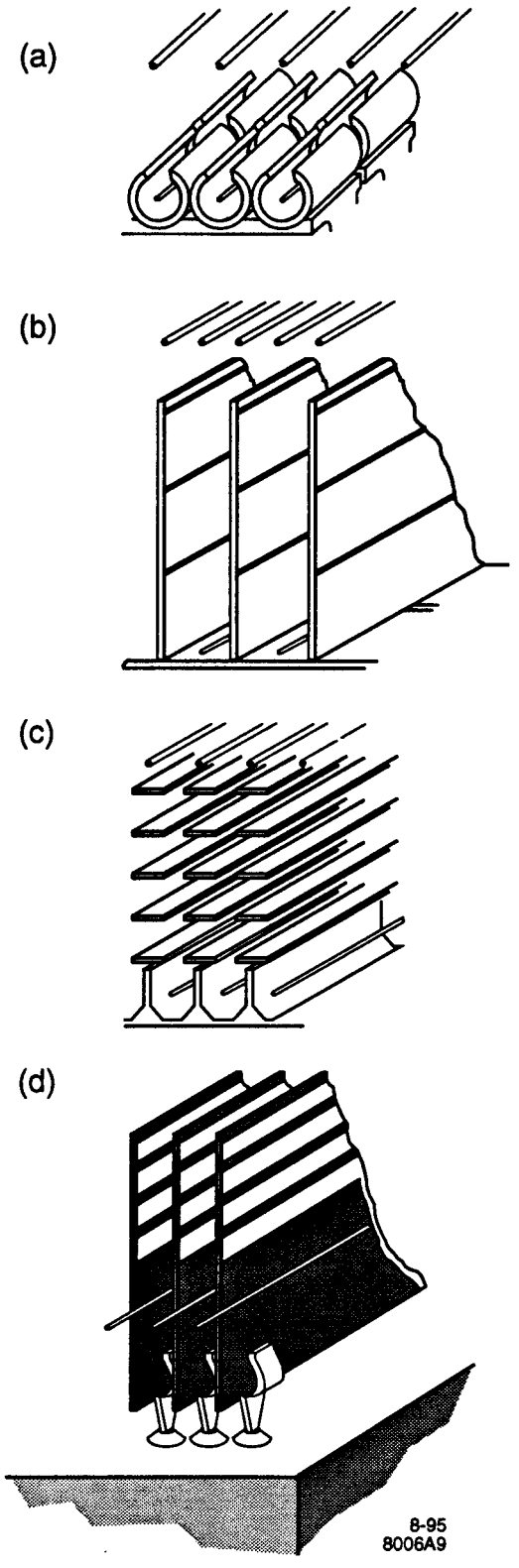

Fig. 4

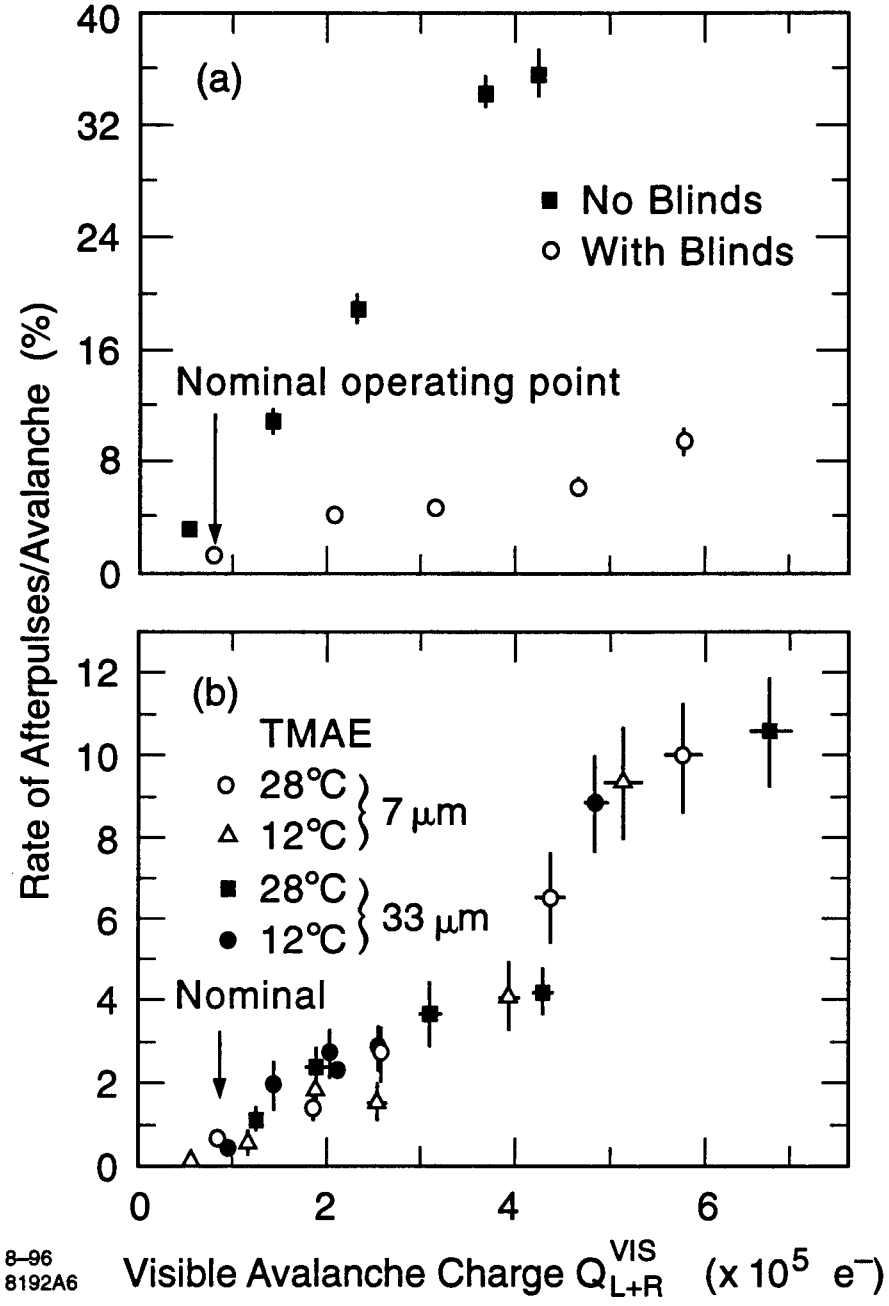
(a)
No Blinds
With Blinds
Nominal operating point
(b)
TMAE
28°C
12°C
7 μm
28°C
12°C
33 μm
Nominal
Rate of Afterpulses/Avalanche (%)
Visible Avalanche Charge Q^{VIS}_{L+R} (x 10^5 e^-)
8-96
8192A6

Fig. 5

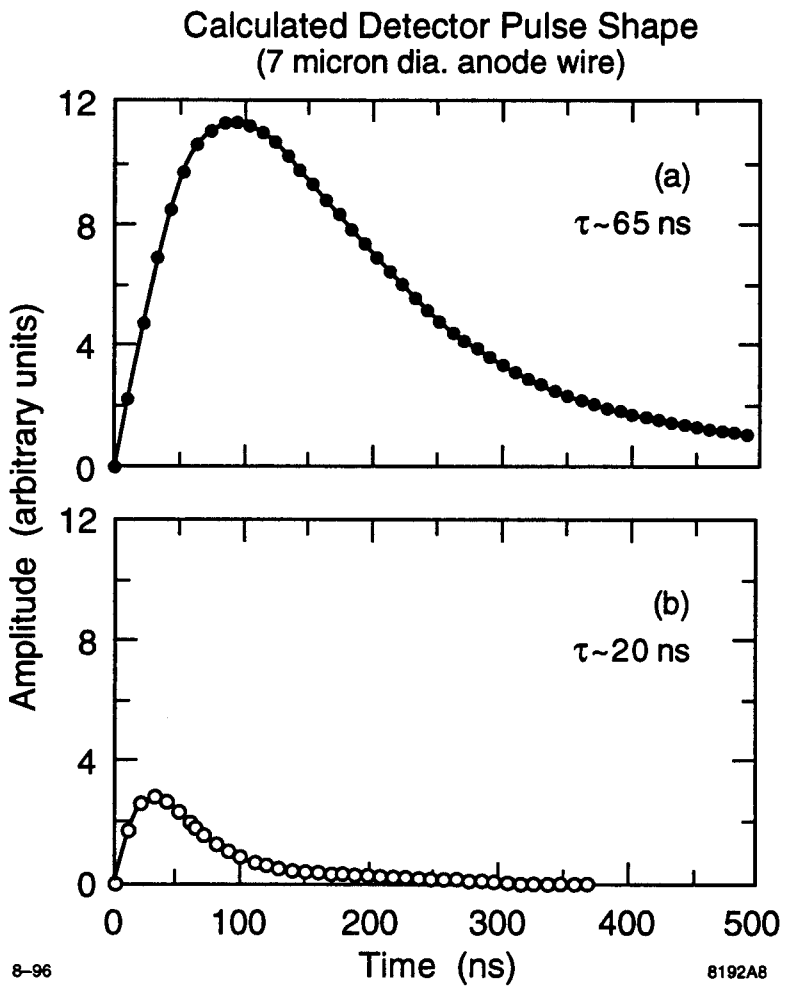
Calculated Detector Pulse Shape
(7 micron dia. anode wire)
12
8
4
0
(a)
τ~65 ns
12
8
4
0
(b)
τ~20 ns
Amplitude (arbitrary units)
0
100
200
300
400
500
Time (ns)
8-96
8192A8

Fig. 6

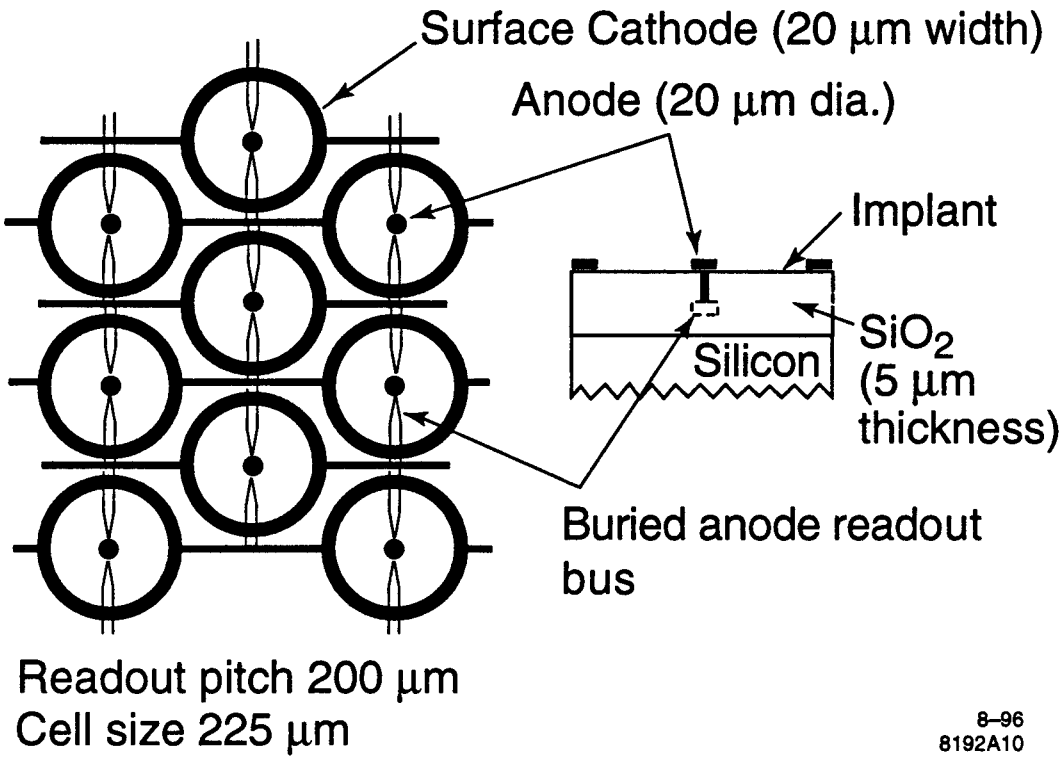
Surface Cathode (20 μm width)
Anode (20 μm dia.)
Implant
SiO_2 (5 μm thickness)
Silicon
Buried anode readout bus
Readout pitch 200 μm
Cell size 225 μm
8–96
8192A10

Fig. 7

(a)

(b)

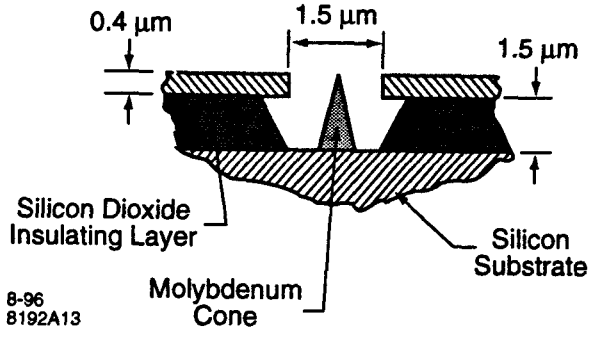
0.4 µm
1.5 µm
1.5 µm
Silicon Dioxide
Insulating Layer
Silicon
Substrate
Molybdenum
Cone
8-96
8192A13

Fig. 8

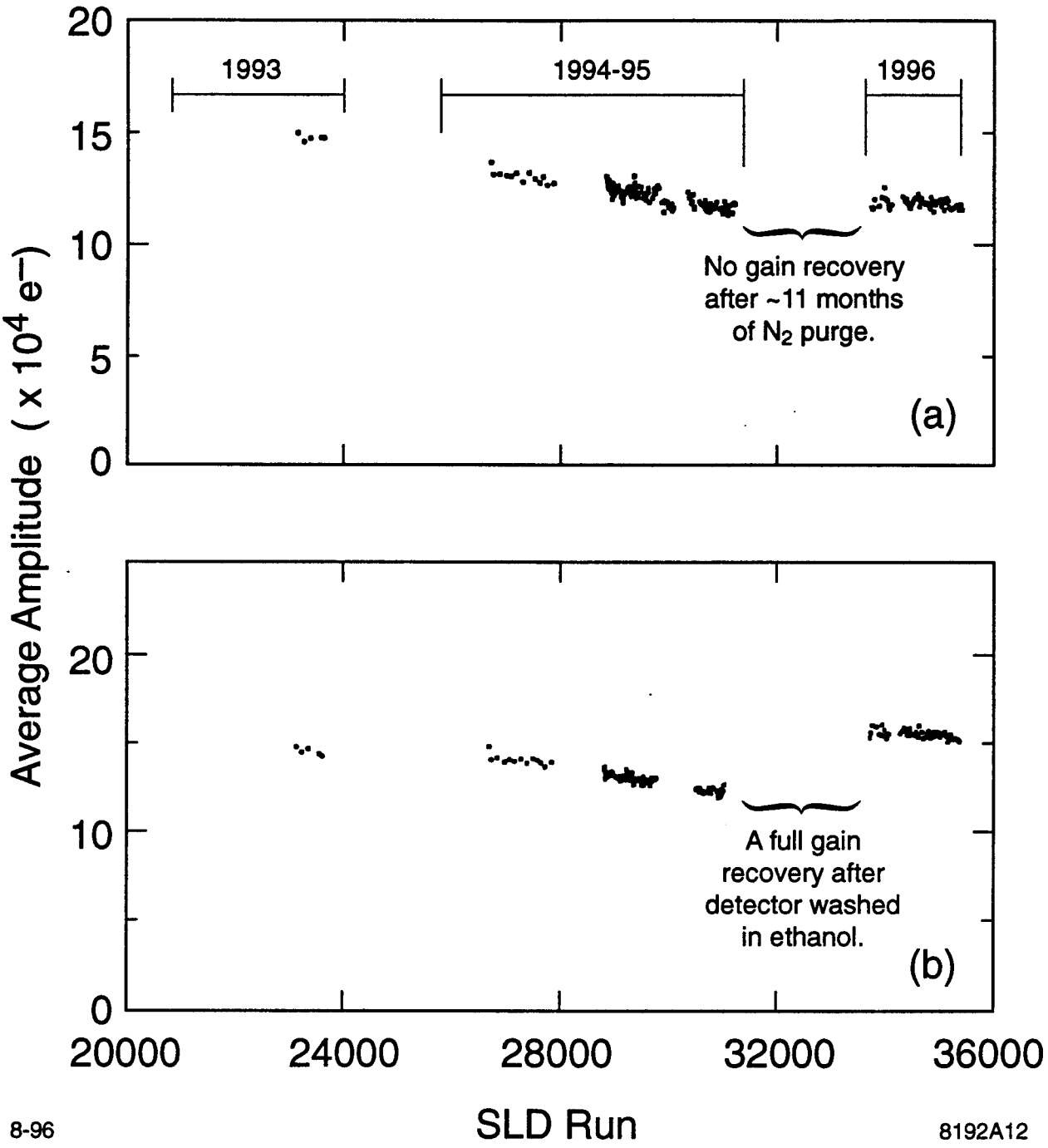
20
15
10
5
0
1993
1994-95
1996
No gain recovery
after ~11 months
of N_2 purge.
(a)
Average Amplitude (x 10^4 e^-)
20
10
0
A full gain
recovery after
detector washed
in ethanol.
(b)
20000
24000
28000
32000
36000
8-96
SLD Run
8192A12

Fig. 9

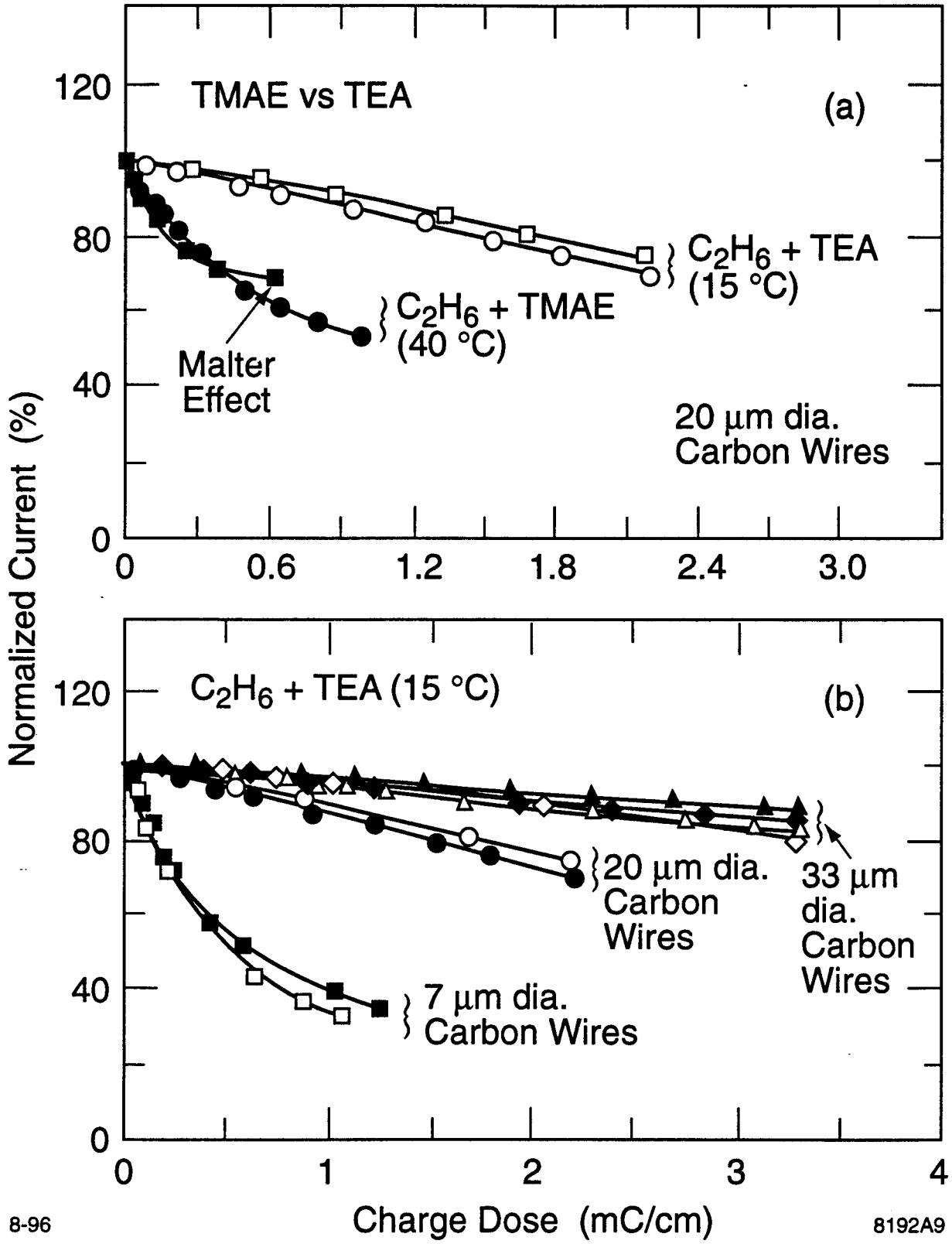
TMAE vs TEA
(a)
120
80
40
0
0
0.6
1.2
1.8
2.4
3.0
C_2H_6 + TEA
(15 °C)
C_2H_6 + TMAE
(40 °C)
Malter
Effect
20 μm dia.
Carbon Wires
Normalized Current (%)
C_2H_6 + TEA (15 °C)
(b)
120
80
40
0
0
1
2
3
4
20 μm dia.
Carbon
Wires
33 μm
dia.
Carbon
Wires
7 μm dia.
Carbon Wires
Charge Dose (mC/cm)
8-96
8192A9

Fig. 10

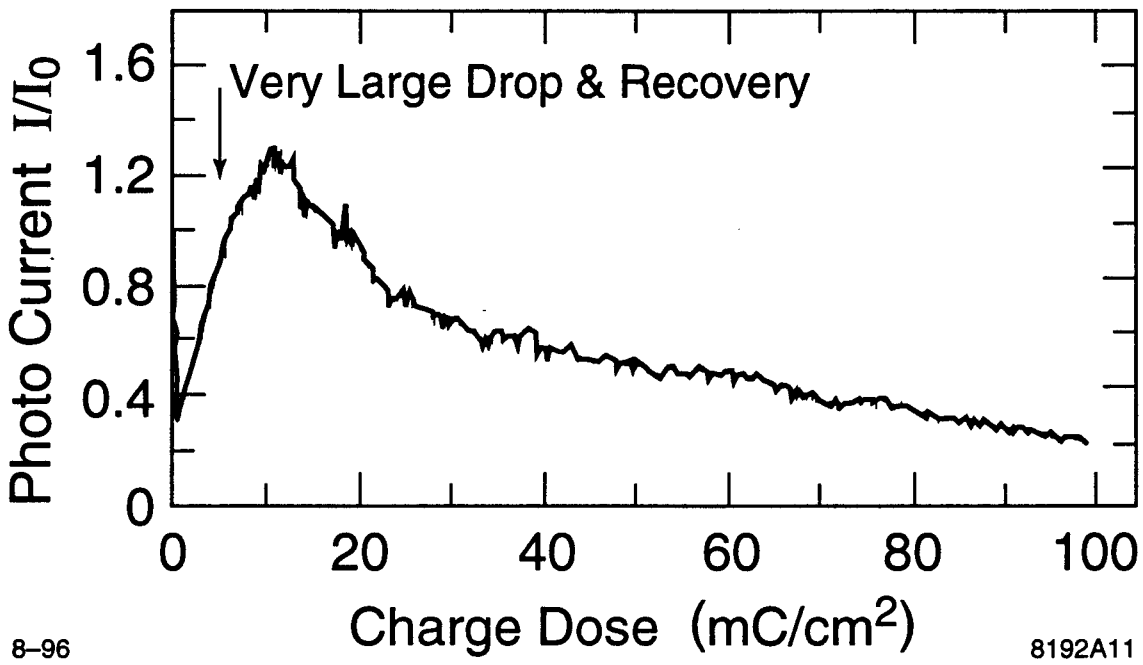
Photo Current I/I_0
1.6
1.2
0.8
0.4
0
Very Large Drop & Recovery
0
20
40
60
80
100
Charge Dose (mC/cm^2)
8–96
8192A11

Fig. 11